

# INTERNATIONAL SOCIETY FOR SOIL MECHANICS AND GEOTECHNICAL ENGINEERING



*This paper was downloaded from the Online Library of the International Society for Soil Mechanics and Geotechnical Engineering (ISSMGE). The library is available here:*

<https://www.issmge.org/publications/online-library>

*This is an open-access database that archives thousands of papers published under the Auspices of the ISSMGE and maintained by the Innovation and Development Committee of ISSMGE.*

# Centrifuge modeling of racking deformations of box culverts



Osama Abuhajar, Hesham El Naggar & Tim Newson

*Department of Civil and Environmental Engineering, Geotechnical Research Center,  
The University of Western Ontario, London, Ontario, Canada*

## ABSTRACT

The response of buried structures subjected to destructive earthquakes has increasingly attracted attention over the last two decades. Some infrastructure have suffered collapse or severe damage in recent earthquakes. Seismic soil-structure interaction is influenced by the relative stiffness between the soil and the buried structure, which also controls the racking deformation defined as the differential sideways movement between the top and bottom slabs of box culverts. The racking ratio between the free field and structural field is of great importance for seismic design of box culverts. In this paper, several small scale model tests were performed on a geotechnical centrifuge and a one-dimensional shaker was used to simulate earthquake shaking events at 60g. These tests were performed to investigate the effect of the box culvert thickness and hosting soil stiffness on the racking deformations. The tests were performed in dry Nevada sand with two relative densities (50 and 90%). The measured acceleration time histories were utilized to determine the displacement time histories and the peak ground displacement (PGD). The calculated displacements were then used to evaluate the racking deformations of the box culverts. Three different earthquakes with different intensities (peak amplitudes) and frequencies were used during testing. The results indicate that the soil density and culvert thickness had significant influence on the observed racking deformations and racking ratios. Reducing the culvert thickness and the soil density resulted in increased racking ratios by a considerable amount compared to culverts that have large slab thickness in very dense sand.

## 1 INTRODUCTION AND LITERATURE REVIEW

Anderson et al. (2008) summarized the general effects of earthquakes on culverts due to ground shaking. Ground shaking refers to the vibration of ground produced by seismic waves (body and surface waves) propagation through the earth's crust. The shaking or travelling waves induce ground deformations that are called transient ground deformations/displacements (TGD). Three types of deformations can happen due to TGD: axial deformations, curvature deformations, and racking deformations. Axial and curvature deformations are unlikely to happen in culverts due to their relatively short lengths. Racking deformations may develop when the waves propagate in perpendicular or nearly perpendicular directions to the longitudinal axis of the buried infrastructure, resulting in a distortion of the shape of the structure. Racking deformations are defined as the differential sideways movements between the top and bottom elevations of rectangular structures. The internal forces can be evaluated by imposing the racking deformation on the structure using a simple frame analysis. The vertically propagating shear waves is the predominant wave form that governs racking because of: (1) ground motion in the vertical direction is less severe than in the horizontal direction, (2) vertical ground strains are generally smaller than shear strains, and (3) the amplification of vertically propagating shear wave is much higher than vertically propagating compression waves.

Wang (1993) developed closed form and analytical solutions for the determination of racking deformations and the corresponding internal forces on tunnel structures based on theory proposed by Peck et al. (1972). This procedure is also applicable to culvert structures.

Hashash et al. (2001) and Anderson et al. (2008) summarized the procedure developed by Wang (1993).

Penzien (2000) presented an analytical procedure for evaluating the racking of rectangular structures during seismic events. This procedure assumes homogenous isotropic soil medium subjected to a uniform shear strain field. Penzien (2000) demonstrated that the deformations of the structure depend on the relative stiffness or the flexibility ratio between the soil and structure.

Hou et al. (2006) presented a closed form solution for rectangular tunnels. This solution accounts for the normal and shear stresses at the interface as well as the actual deformations of a rectangular opening. Complex variable theory and conformal mapping were used assuming a plane strain deep rectangular structure in a homogenous, isotropic and elastic medium. This solution can be used for pseudo-static analysis, where the seismic deformations of the soil and structure can be approximated through far-field shear stress or strain.

Hou et al. (2006) stated that in the free field approach, the structure must accommodate the free field deformations without loss of integrity and this may not be correct. This is because for a structure that is more rigid than the soil, the structure will reduce the deformations from the surrounding soil. If the structure is more flexible than the soil, the linear distortions are larger than the free field deformations.

Bobet et al. (2008) used the analytical solution by Hou et al. (2006) and proposed a procedure to incorporate the soil stiffness degradation through an iterative process, where the soil shear modulus is changed in each iteration based on the shear strain of the soil obtained in the previous iteration. The process ends when the shear

modulus used in the last iteration corresponds to the soil deformation.

Nishioka and Unjoh (2003) proposed a simplified method based on the shear deformation capacity. They investigated the shear deformation capacity using nonlinear finite element analyses of five types of standard boxes. In the evaluation method, the seismic performance is assessed from the difference between the soil strain and the peak soil strain at the structure level. The results show that the boxes can have enough ductility with respect to the shear deformations. It was noted also that as the thickness of the structure increases, the shear strains decrease.

Wood (2005) used the method proposed by Wang (1993) to analyze single and double barrel structures on soils and rocks. Wood (2005) compared the results obtained for the racking ratio and flexibility ratio with the simplified method proposed by Nishioka and Unjoh (2003) and the analytical method proposed by Penzien (2000). They reported good agreement between all of the methods, particularly for a flexibility ratio less than 2.0.

Amiri et al. (2008) used the analytical method proposed by Penzien (2000) and performed a parametric study employing FEM to assess the effect of structure geometry and embedment depth ( $h/H$ ), where  $h$  is the height from ground surface to the mid-side of the structure height and  $H$  is the height of the structure. The results showed that the racking deformations are insensitive to the structure geometry, and that the racking deformation is independent of embedment depth, for burial ratios  $h/H > 2$ . For stiffer structures than the soil and  $h/H < 2$ , the racking distortion decreases as the burial depth decreases, while for flexible structures with  $h/H < 2$ , the racking increases as the depth decreases.

Katona (2010 a and b) presented a step by step methodology for analyzing and evaluating the structural integrity of a buried structure under the combined influence of static and seismic loading. The analysis combined the racking procedure proposed by Wang (1993) and the CANDE-2007 software developed by the Katona. Using CANDE-2007, a plane strain finite element program, the soil structure problem can be characterized. In static design, loads are applied with a series of incremental load steps. Then, the seismic loading is simulated by specifying quasi-static displacements at the peripheral boundaries of the soil envelope, to produce shear racking distortion equivalent to the maximum free field seismic shear strain from the design earthquake. The procedure applies to any culvert shape, size, material, and the design can be assessed either by working stress (WS) or load reduction factor design (LRFD).

Recent studies investigated the racking ratio using centrifuge and numerical modeling. Ulgen et al. (2015a) compared the centrifuge test results and Penzien's estimates and suggested that the racking ratios were underestimated by a factor of nearly 1.5–2 using Penzien's approach. This discrepancy may be attributed to ignoring the dynamic soil pressures. Racking ratios obtained from centrifuge tests are overestimated by roughly a factor between 2 and 3 using the method of Bobet et al. (2008). Thus, the racking deformation calculated by the approach proposed by Bobet et al.

(2008) may be used as a conservative estimate for preliminary design of rectangular underground structures embedded in dry sand. Ulgen et al. (2015b) investigated the use of readings from accelerometers and extensometers to calculate the racking ratio in centrifuge tests. Racking ratios calculated from the records of accelerometers are relatively higher than those obtained by extensometers. It is believed that such differences are caused by the existence of rocking motion.

Tsinidis et al. (2014) performed centrifuge tests to investigate the racking ratio and the results indicated that the tunnel behaves as a rigid structure with respect to the surrounding soil, as the structural distortions are decreased with respect to the soil. This behavior is not consistent with the results of the analytical procedure proposed by Wang (1993) for the estimation of the relative soil to structure flexibility.

Tsinidis et al. (2015) compared the racking ratios from different methods to the dynamic analysis using centrifuge results. The racking ratio results show that the dynamic analysis is slightly larger than the other methods by 15 – 20% for flexible tunnels. For rigid tunnels, Wang (1993) overestimates the racking ratio. The overestimation of the racking ratio may lead to an overdesign that may be considered as a conservative 'safe' design concept. However, overdesign is not only needlessly expensive but may lead to the stiffening of the structure, which may in turn change the whole response pattern in a detrimental way.

In this paper, the results of racking deformations and racking ratio based on centrifuge modeling of box culverts with two different thicknesses and two different relative densities of dry Nevada sand are presented. The results show that there is a significant combined effect for the culvert thickness and soil density on the values of racking ratio and deformations.

## 2 CENTRIFUGE MODELING

### 2.1 Box Culvert Model

A square aluminum tube with a 76 mm side length was selected to represent a 4.5 m culvert at 60g in the centrifuge tests, considering the dimensions of box culverts used in practice. Previous studies have used different materials to model the behaviour of reinforced concrete box culverts, such as mild steel (Stone et al., 1991) and aluminum (Stone and Newson, 2002). This is due to the difficulties involved in constructing model culverts from a micro-concrete aggregate with appropriate reinforcement. The scaling law proposed by Stone et al. (1991) was used to determine the thickness and stiffness properties of the box culvert as shown in this relationship:

$$t_p = nt_m a^{1/3} \quad [1]$$

where  $t$  = wall thickness, and  $a = E_m/E_p$ ,  $E$  = Young's modulus of the material, and  $n$  = scaling factor. The

subscripts 'm' and 'p' refer to model and prototype, respectively.

To maintain the scaling laws, the model culvert (shown in Figure 1) was made from an aluminum square section with an external dimension of 76.2 mm (3 inch) and two wall thicknesses; thick walled  $t = 6.35$  (1/4") and thin walled  $t = 3.18$  (1/8") mm.

## 2.2 Centrifuge Model Tests

The centrifuge model testing was conducted at the RPI centrifuge facility. The centrifuge model was prepared by placing the sand into a rectangular rigid box with dimensions of 863.6 mm long x 381 mm wide x 355.6 mm high. Dry 120-Nevada Sand was used for all of tests. This is a uniform sand classified according to USCS as a poorly graded sand (SP) with a  $d_{10} = 80 \mu\text{m}$  and maximum and minimum densities of 1.71 and 1.51  $\text{g/cm}^3$ , respectively.

To achieve the required relative densities, Nevada Sand was placed in layers by air pluviation for 50% relative density; while for 90% relative density each sand layer was tamped after air pluviation. Figure 2 shows a schematic diagram of the centrifuge model including the box culvert with the sand bed.

The box culvert model was instrumented with accelerometers at different positions inside the sand and around the box culvert to measure the change in the acceleration time history during shaking as shown in Figure 2. The accelerometers Ac2, Ac3, Ac4, Ac5 and Ac6 were used to measure the horizontal acceleration time history inside the sand body along a vertical section away from the structure (box culvert). This was assumed to be the Free Field (FF) condition. On the other hand, the accelerometers Ac7, Ac8, Ac9, Ac12, and Ac13 were used to measure the horizontal acceleration time history along a vertical section in the area of the box culvert, and therefore, were defined as the Structure Field (SF) condition.

After building the model, the one-dimensional shaker was placed on the centrifuge platform and then the centrifuge model box was placed over it. All accelerometers were checked and connected to the data acquisition system. The centrifuge accelerated incrementally and at 60g, all of the earthquake signals were sent to the shaker.

Each test included three cases. Case A: with sand only, Case C: with a surface strip foundation positioned right over the box culvert location, and Case D: with surface rectangular foundation centrally positioned right over the box culvert location.

## 2.3 Earthquake Records

Figure 3 shows the one-dimensional shaker that was used to apply the earthquake records to the centrifuge box model. The shaker has a displacement-controlled actuator, and does not directly accept acceleration time histories of earthquake records as input. Therefore, all earthquake records were scaled to voltage, and sent to the shaker as an electric signal.

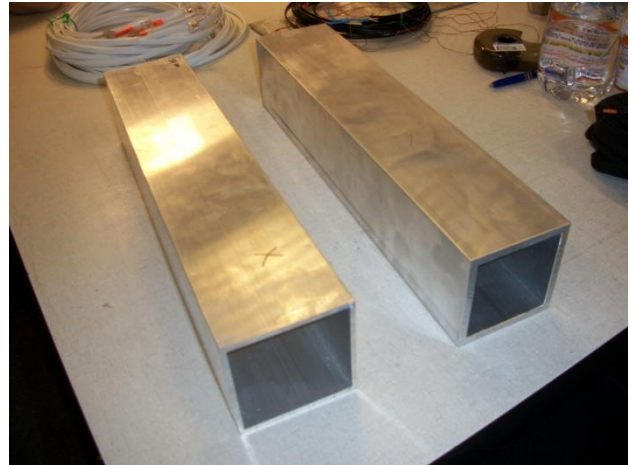


Figure 1. Box culvert models.

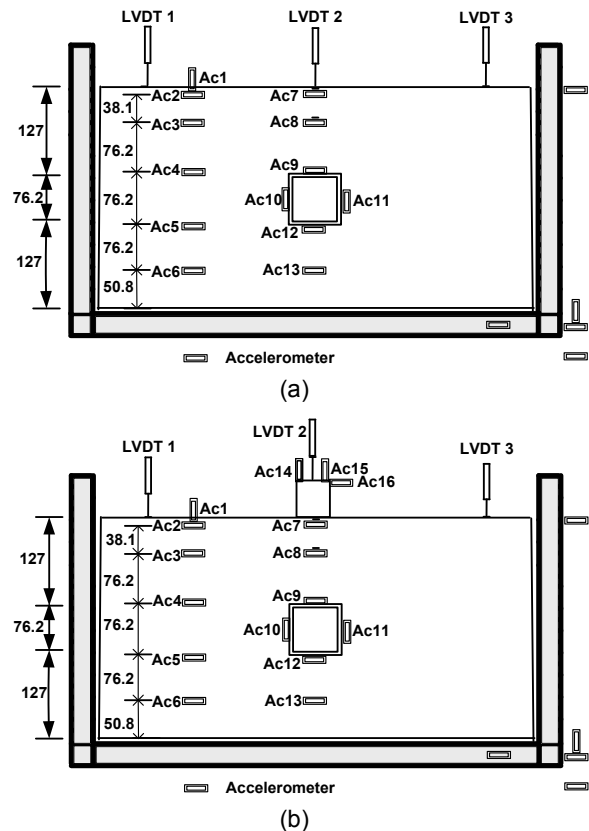


Figure 2. Schematic diagram for centrifuge tests. (a) No foundation, (b) With foundation. (All units are in mm)

The response of the shaker to this signal would be in the form of displacement that can be measured using a Linear Variable Differential Transducer (LVDT). To ensure that the voltage signal sent to the shaker matches closely the earthquake record, an accelerometer was connected to the shaker to monitor and record the acceleration time history and then compared it to the original earthquake record. Additionally, the displacement recorded by the

LVDTs were compared to the displacement time history calculated by double integrating the acceleration time history recorded from the shaker.

It is also important to compare the acceleration time history recorded from the shaker and that of the base of the centrifuge box, which was considered to be the earthquake record applied to the tested model.

To ensure that all of the earthquake records used in these tests had the target amplitude and frequency, a dummy test was conducted before starting the actual tests. In the dummy test, an equivalent model was built and subjected to all earthquake records with different amplitudes. The results of the dummy test were used to establish a relationship between the voltage values and the amplitudes recorded to establish the values of voltage that give the required level of shakings.

Three different earthquakes with different amplitudes and frequencies were adopted for use in these series of tests. These earthquakes are: the Kobe earthquake (North-East component of the Port Island down hole array -79 m record), Western Canada, and Vancouver Cascadia Subduction (Artificial records corresponding to 2% probability of occurrence in 50 years). The predominant frequencies of these earthquakes are 1.453, 0.647, and 0.464 Hz, respectively. It was challenging for the shaker to provide an exact match for the original shapes of these earthquakes and therefore a process of filtering and trial and error was applied on the dummy models until a good match was found between the filtered records and the response at the base of each centrifuge box model. The final form of the filtered earthquakes that were used in all tests are shown in Figure 4. The records shown in Figure were scaled to 0.1g. However, the records were scaled up to 0.2g and 0.3g for different tests.

Another important aspect that might affect the results obtained from the accelerometers utilized in the centrifuge tests was the effect of centrifuge box boundaries. Since the box used in the tests was rigid, the boundary effect was investigated during the dummy test. Several accelerometers were distributed in the sand bed at the same elevation and different distances from the boundary, and also on the centrifuge box to examine the boundary effect. The recorded acceleration time histories from all accelerometers within the sand bed were compared. The results showed that there was no effect from the boundary on the results. The acceleration time history recorded from the accelerometers that were positioned at the same elevation and at different distances from the box side gave almost the same results. It should be noted that the closest accelerometer to the box side was placed at 3 mm from the sides of the centrifuge box. It should also be noted that the box walls were not very thick (7 mm model scale or 420 mm at 60g) (Abuhajar, et al. 2013, 2015a, 2015b and 2016).

### 3 CENTRIFUGE RESULTS

Wang (1993) proposed a procedure to determine the racking deformations of the differential movement of the top and bottom slabs of the culvert using the racking ratio. Following this procedure, the peak ground displacements

were used to calculate the change in free field ( $PGD_{FF}$ ) and the structure field peak ground displacement ( $PGD_{SF}$ ), i.e.:



Figure 3. One Dimensional Box Shaker at RPI.

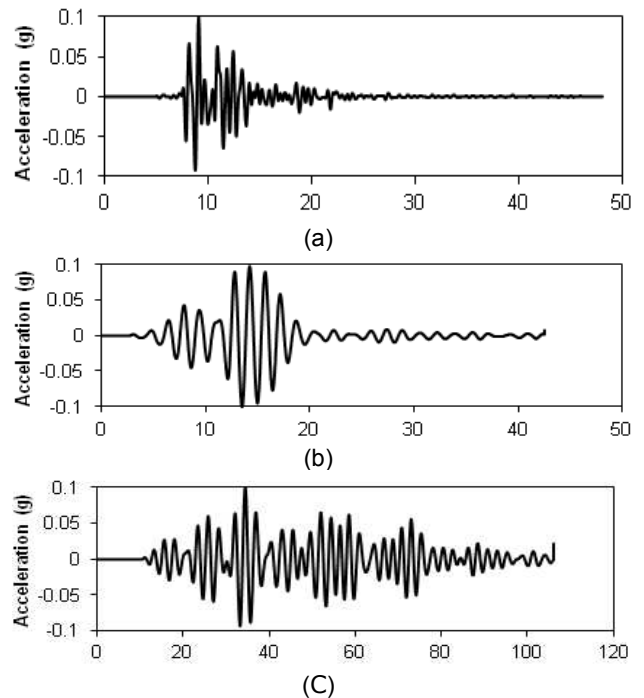


Figure 4. Time histories for the: (a) Kobe, (b) Western Canada and (c) Vancouver Cascadia earthquakes.

$$\Delta PGD_{FF} = PGD_4 - PGD_5 \quad [2]$$

$$\Delta PGD_{SF} = PGD_9 - PGD_{12} \quad [3]$$

where  $PGD_4$ ,  $PGD_5$ ,  $PGD_9$  and  $PGD_{12}$  are peak ground displacements at the levels of the culvert top and bottom slabs, which were obtained by double integrating the horizontal acceleration time histories of  $Ac_4$ ,  $Ac_5$ ,  $Ac_9$  and  $Ac_{12}$ .

The racking ratio  $R$  is then calculated as:

$$R = \frac{\Delta PGD_{SF}}{\Delta PGD_{FF}} \quad [4]$$

The racking ratios obtained from Tests 1, 2, 3, and 4 are presented in Tables 1, 2, 3 and 4. Generally, most of the differences in  $PGD$  either in Free Field (FF) or Structural Field (SF) are positive, which indicates that the  $PGD$  at the level of top slab is larger than that at the level of the bottom slab. Only some shaking cases in Test 3 exhibited a negative sign in the FF indicating the opposite. The results presented in the tables show that the thickness of the culvert and sand density can affect the racking ratio (i.e. cumulative effect).

### 3.1 Effect of soil density

The results of Tests 1 and 2 clearly show the racking ratios of the thick culvert for cases of  $Dr = 90\%$  and  $50\%$ . The racking ratios for Test 1 are in the range of 0.1 and 0.7, which indicates that the racking deformation of the culvert for the SF is less than that for the FF. On the other hand, the racking ratios for Test 2 are in the range of 1.5 to 1.9, which indicates an increase in the culvert deformations for the SF over those for the FF.

Comparing the results of Tests 3 and 4, which are for the thin culvert at  $Dr = 50\%$  and  $90\%$ , shows that combining the lower density with a thin culvert in Test 3 produces a high racking ratio ranging from -8 to 156, while for Test 4 the range was between 5 and 13 depending on the test case and level of shaking. In both tests, the racking deformations of the SF are higher than those for the FF.

### 3.2 Effect of culvert thickness

The results of Tests 1 and 4 (as well as Tests 2 and 3) are compared to investigate the effect of culvert thickness. The results of Tests 1 and 4 for  $Dr = 90\%$ , and Tests 2 and 3 for  $Dr = 50\%$ , show that the thick culvert experienced very small racking deformations compared to the thin culvert. It may be concluded that the level of racking deformations in the thick (i.e. more rigid) culverts are less than for thin (i.e. less rigid) culvert.

Comparing the extreme cases of Test 1 and Test 3, it is noted that culvert racking in Test 1 is the lowest. This is because of the culvert high rigidity and soil high density, the culvert and soil move together during shaking, which reduces the racking deformations of the culvert. On the other hand, the racking in Test 3 is the highest. This is because the culvert is flexible and the soil is not dense, the culvert elements will move with shaking resulting in high racking deformations. In addition, the racking ratio for the FF in some shakings in Test 3 were negative, which indicates that using FF deformations can sometime correctly predict the culvert behaviour under seismic loading in similar situations. The results show that, as expected, the culvert racking deformations increase as the level of shaking increases and that the relative stiffness between the culvert and soil appears to have a great effect.

### 3.3 Flexibility ratio

The flexibility ratio ( $F$ ) represents the relative stiffness between the box culvert and the surrounding sand, which is an important factor in studying the soil culvert interaction. As this research investigates two different thicknesses and two different relative densities, their values can have an effect on the values of the flexibility ratio. The calculated values of the flexibility ratios for both culvert thicknesses and soil densities show a wide range of values. For the thick culvert, the flexibility ratios are 0.1 and 0.3, while for the thin culvert, the flexibility ratios are 0.8 and 2.3 for the 50% and 90% relative densities respectively.

According to Wang (1993), if  $F < 1.0$ , the structure is considered stiff relative to the soil and will therefore deform less, while if  $F > 1.0$ , the racking distortion of the structure is amplified relative to the free field. This is not due to dynamic amplification but because the soil now has a cavity, providing lower shear stiffness than the free field. The results presented in Tables 1 to 4 are in good agreement with the above flexibility values.

It was observed from the results of the thin culvert with a flexibility ratio of 0.8 (thin culvert with 50% relative density) that the racking distortion for the structural field is higher than the racking distortion for the free field and this causes higher values for the racking ratios. For the case of the thin culvert with a flexibility ratio of 2.3 (thin culvert with 90% relative density), similar observation but with lesser values of racking distortion for the structural field was found. This lead to lower values of racking ratios. For the thick culvert, both flexibility ratios are consistent with the values presented by Wang (1993).

## 4. CONCLUSION

The racking deformations are widely used for seismic design of box culverts (Wang, 1993) and this procedure can be used for pseudo-static analysis. The racking ratio of the box culvert (which represents the ratio between the differential movements at the top and bottom slabs for the Free Field and Structural Field) was investigated based on the centrifuge test results. The centrifuge results of racking deformations in box culverts indicate that the racking deformation may be different than that suggested by the racking method. In the case of a box culvert with thick walls installed in very dense sand, the racking ratio was less than 1.0, which indicates that the deformations for the free field are higher than those for the structure field. For the other cases where the soil is medium dense with a thick-wall culvert or the culvert wall is thin (irrespective of density), the racking ratio is larger than 1.0 and in some cases very high. This proves that the racking deformations for the structure field could be much higher than for the free field. In some cases, the difference between the deformations at the top and bottom slabs of the culvert and in the free field are negative, which indicates that the values at the top are less than those at the bottom.

Recent studies that investigated the racking ratios using centrifuge modeling were presented. The focus of

all of this previous work was on specific thicknesses of culvert in a specific soil density. The contribution in this paper is that the effect of different culvert thicknesses and different soil densities were investigated in the centrifuge modeling.

The results obtained are very significant and indicate that the racking ratios for flexible culverts should be investigated thoroughly for safe and economic design.

Table 1. Racking of the box culvert in Test 1

Test	EQ	PGA (Base) (g)	$\Delta PGD_{FF}$ (cm)	$\Delta PGD_{SF}$ (cm)	$\frac{\Delta PGD_{SF}}{\Delta PGD_{FF}}$
T1A	WCL	0.089	0.13	0.06	0.52
T1C	WCL	0.097	0.12	0.07	0.56
T1A	WCM	0.241	0.17	0.13	0.73
T1C	WCM	0.240	0.14	0.13	0.98
T1A	VCL	0.103	0.20	0.02	0.09
T1C	VCL	0.113	0.22	0.03	0.13
T1A	VCM	0.164	0.28	0.09	0.31
T1C	VCM	0.170	0.25	0.07	0.30
T1A	KEQL	0.122	0.12	0.09	0.76
T1C	KEQL	0.098	0.09	0.07	0.78
T1A	KEQM	0.205	0.21	0.16	0.77
T1C	KEQM	0.203	0.18	0.13	0.76
T1A	KEQH	0.308	0.18	0.08	0.46
T1C	KEQH	0.319	0.14	0.04	0.31

Table 2. Racking of the box culvert in Test 2

Test	EQ	PGA (Base) (g)	$\Delta PGD_{FF}$ (cm)	$\Delta PGD_{SF}$ (cm)	$\frac{\Delta PGD_{SF}}{\Delta PGD_{FF}}$
T2A	WCL	0.097	0.38	0.60	1.57
T2C	WCL	0.109	0.39	0.65	1.67
T2A	WCM	0.227	0.61	0.96	1.57
T2C	WCM	0.239	0.58	0.94	1.63
T2A	VCL	0.113	0.66	1.30	1.97
T2C	VCL	0.119	0.71	1.39	1.95
T2A	VCM	0.183	0.95	1.70	1.79
T2C	VCM	0.195	0.93	1.74	1.86
T2A	KEQL	0.105	0.25	0.36	1.45
T2C	KEQL	0.101	0.27	0.44	1.59
T2A	KEQM	0.201	0.49	0.85	1.73
T2C	KEQM	0.200	0.49	0.85	1.74
T2A	KEQH	0.333	0.53	0.90	1.69
T2C	KEQH	0.306	0.55	0.94	1.72

Table 3. Racking of the box culvert in Test 3

Test	EQ	PGA (Base) (g)	$\Delta PGD_{FF}$ (cm)	$\Delta PGD_{SF}$ (cm)	$\frac{\Delta PGD_{SF}}{\Delta PGD_{FF}}$
T3A	WCL	0.108	0.03	0.65	23.51
T3C	WCL	0.107	0.03	0.62	24.67
T3D	WCL	0.110	0.01	0.62	57.32
T3A	WCM	0.240	0.08	1.01	12.35
T3C	WCM	0.242	0.03	0.96	36.64
T3D	WCM	0.252	0.02	0.97	54.29
T3A	VCL	0.118	-0.15	1.32	-8.85
T3C	VCL	0.125	-0.14	1.30	-9.56
T3D	VCL	0.135	-0.16	1.32	-8.48
T3A	VCM	0.184	-0.09	1.73	-19.49
T3C	VCM	0.181	-0.06	1.64	-29.31
T3D	VCM	0.189	-0.08	1.71	-22.12
T3A	KEQL	0.113	0.07	0.44	6.11
T3C	KEQL	0.098	0.03	0.45	14.52
T3D	KEQL	0.104	0.04	0.43	11.24
T3A	KEQM	0.214	0.06	0.92	15.92
T3C	KEQM	0.201	-0.02	0.87	-45.60
T3D	KEQM	0.203	-0.01	0.86	-158.50
T3A	KEQH	0.313	0.02	1.02	48.13
T3C	KEQH	0.298	-0.01	1.00	-91.82
T3D	KEQH	0.301	0.01	0.98	156.03

Table 4. Racking of the box culvert in Test 4

Test	EQ	PGA (Base) (g)	$\Delta PGD_{FF}$ (cm)	$\Delta PGD_{SF}$ (cm)	$\frac{\Delta PGD_{SF}}{\Delta PGD_{FF}}$
T4A	WCL	0.103	0.12	0.70	6.07
T4C	WCL	0.103	0.13	0.69	5.50
T4D	WCL	0.108	0.13	0.73	5.52
T4A	WCM	0.205	0.12	0.94	8.15
T4C	WCM	0.211	0.15	0.95	6.20
T4D	WCM	0.222	0.15	1.01	6.77
T4A	VCL	0.117	0.10	1.42	13.96
T4C	VCL	0.115	0.12	1.42	11.41
T4D	VCL	0.137	0.15	1.55	10.71
T4A	VCM	0.169	0.17	1.63	9.39
T4C	VCM	0.174	0.20	1.64	8.29
T4D	VCM	0.186	0.19	1.81	9.52
T4A	KEQL	0.122	0.12	0.55	4.77
T4C	KEQL	0.105	0.12	0.51	4.20
T4D	KEQL	0.104	0.10	0.50	4.86
T4A	KEQM	0.189	0.14	0.91	6.27
T4C	KEQM	0.179	0.13	0.91	7.23
T4D	KEQM	0.186	0.13	0.96	7.32
T4A	KEQH	0.266	0.14	1.02	7.07
T4C	KEQH	0.271	0.16	1.10	6.81
T4D	KEQH	0.270	0.17	1.10	6.34

## 5. REFERENCES

- Abuhajar O.S. 2013 Static and seismic soil culvert interaction. London, ON: Department of Civil and Environmental Engineering, The University of Western Ontario
- Abuhajar, O.S., El Naggar M.H and Newson, T., 2015a. Seismic soil culvert interaction. *Canadian Geotechnical Journal*, 52(11), 1649-1667
- Abuhajar, O.S., El Naggar M.H and Newson, T., 2015b. Experimental And Numerical Investigations Of The Effect Of Buried Box Culverts On Earthquake Excitations. *Soil Dynamics and Earthquake Engineering Journal* (79): 130 – 148
- Abuhajar, O.S., El Naggar M.H and Newson, T., 2016. Interpreting dynamic soil properties of dry Nevada sand from centrifuge modeling. The 3<sup>rd</sup> European conference on Physical Modeling in Geotechnics (Eurofuge 2016)
- Amiri, G.G., Maddah, N. and Mohebi, B. 2008. Effective parameters on seismic design of rectangular underground structures. *In Proceedings of Seismic Engineering Conference Commemorating the 1908 Messina and Reggio Calabria Earthquake*, American Institute of Physics, pp 719-725
- Anderson, D.G., Martin, G.R., Lam, I., and Wang, J.N. 2008. Seismic analysis and design of retaining walls, buried structures, slopes and embankment. NCHRP Rep. No. 611, TRB, National Research Council, Washington, D.C.
- Bobet, A. Fernandez, G. and Ramirez, J. 2008. A practical iterative procedure to estimate seismic-induced deformations of shallow rectangular structures. *Canadian Geotechnical Journal* 45: pp. 923–938
- Hashash, Y.M.A., Hook, J.J., Schmidt, B., Yao, J.I., 2001. Seismic design and analysis of underground structures. *Tunneling and Underground Space Technology* 16, 247–293.
- Huo, H., Bobet, A., Fernández, G., and Ramírez, J. 2006. Analytical solution for deep rectangular underground structures subjected to far-field shear stresses. *Tunnelling and Underground Space Technology*, 21: 613–625. doi:10.1016/j.tust.2005.12.135.
- Kanungo, M. 2008. Soil-Structure Interaction for Buried Box Culverts. M.Sc. thesis, the University of Western Ontario.
- Katona, M.G. 2010a. Seismic design and analysis of buried culverts and structures. *Journal of pipeline systems engineering and practice*, Vol. 1 No. 3 pp 111-119
- Katona, M.G. 2010b. Seismic design and analysis of buried structures with CANDE-2007. *Journal of Transportation Research Board*, No. 2172 pp 171-181
- Nishioka, T. and Unjoh, S. 2003. A simplified evaluation method for the seismic performance of underground common utility boxes. *In Proceedings of Pacific Conference on Earthquake Engineering*, Paper No. 55
- Peck, R.B., Hendron, A.J. and Mohraz B. 1972. State of the Art of Soft Ground Tunnelling. *In Proceedings of the Rapid Excavation and Tunneling Conference*, Chicago, IL, Vol. 1.
- Penzien, J., 2000. Seismically induced raking of tunnel linings. *Earthquake Engineering and Structure Dynamics* 29, 683–691.
- Tsinidis G., Heron C., Pitilakis K. and Madabhushi G. 2014. Physical Modeling for the Evaluation of the Seismic Behavior of Square Tunnels. A. Ilki and M.N. Fardis (eds.), *Seismic Evaluation and Rehabilitation of Structures*, Geotechnical, Geological and Earthquake Engineering 26, Springer International Publishing Switzerland.
- Tsinidis G., Pitilakis K., Madabhushi G. and Heron C. 2015. Dynamic response of flexible square tunnels: centrifuge testing and validation of existing design methodologies. *Geotechnique* 65, No. 5, 401-417.
- Ulgen, D., Saglam, S. and Ozgan M.Y. 2015a. Assessment of racking deformation of rectangular underground structures by centrifuge tests. *Geotechnique Letters* 5, 261-268.
- Ulgen, D., Saglam, S. and Ozgan M.Y. 2015b. Dynamic response of a flexible rectangular underground structure in sand: centrifuge modeling. *Bull Earthquake Eng* (2015) 13:2547–2566.
- Wang, J., 1993. *Seismic Design of Tunnels - A Simple State-of-the-Art Design Approach*. William Barclay Parsons Fellowship, Parsons Brinckerhoff, Monograph 7.
- Wood, J.H. 2005. Earthquake design of rectangular underground structures. *New Zealand Society for Earthquake Engineering Conference*, Paper No. 39